ZIRCONIUM BASED METAL ORGANIC FRAMEWORK DEPOSITED ONTO MODIFIED ALUMINA HOLLOW FIBER FOR HUMIC ACID REMOVAL

NORFAZLIANA BINTI ABDULLAH

UNIVERSITI TEKNOLOGI MALAYSIA

ZIRCONIUM BASED METAL ORGANIC FRAMEWORK DEPOSITED ONTO MODIFIED ALUMINA HOLLOW FIBER FOR HUMIC ACID REMOVAL

NORFAZLIANA BINTI ABDULLAH

A thesis submitted in fulfillment of the
requirements for the award of the degree of
Doctor of Philosophy

School of Chemical and Energy Engineering
Faculty of Engineering
Universiti Teknologi Malaysia

JULY 2021

ACKNOWLEDGEMENT

Bismillahirrahmanirrahim,

Praise to Allah The Almighty, who gives all the opportunities and strengths for the completion of this thesis. I would like to convey the honor to my dedicated supervisor, Assoc. Prof. Dr. Mukhlis A. Rahman for his guidance, supervision, and friendship throughout my Doctoral Philosophy (PhD) study. His great assistance contributes to the ideas of my research study. Without his passion and determination, this thesis would not have presented as written here.

I am also indebted to the School of Graduate Studies for the financial support of Zamalah Scholarship for my entire study. Ministry of Higher Education for their research fund and financial allocation also deserve special appreciation. Endless thank you to my research team fellows including Nor Azureen, Syafikah Huda, Norfadhilatuladha, Faten Ermala, Siti Nur Fatin Nadhirah, Intan Nuralisa, Zhatul Shima, Norfazilah, Mohamad Zahir, Nizar Muammar, Muhamad Amirul Afiat, Naziha, Noradila, and AMTEC fellows. I appreciate the time we work together, especially for your supportive encouragement.

Special thanks to all members of the Postgraduate Student Society of School of Chemical and Energy Engineering (SCEE) for batch 2017/2018 and 2018/2019 under the advice of Assoc. Prof. Dr. Muhammad Manan and Assoc. Prof. Dr. Zurina whose helped in the development of my soft skills. Not forgotten, thank you so much to the administrations of SCEE and Faculty of Engineering (FE) for their assistance.

I am also would like to appreciate the help received from research officers, Mr. Ng Bee Cher, Mr. Sohaimi, Mr. Razis, Mr. Hanis, Mr. Arif, and Mr. Nizam. Their expertise contributed to the completion of my PhD study. Thank you to AMTEC research center that created a conducive research environment, provided infrastructures, research facilities, and a platform to involve in any events management.

ABSTRACT

Membrane technology using alumina hollow fiber (AHF) deposited with zirconium-based metal-organic framework (MOF) known as UiO-66 serves as a great option for humic acid (HA) removal present in water systems. The main limitation for growing UiO-66 on AHF is the difficulty to develop a well-continuous and defect-free UiO-66 layer onto AHF due to its abundant micropores and tubular configuration, resulting in low stability and poor HA rejection. There are three objectives of this study which are i) to study the single deposition and second deposition of UiO-66 membrane onto AHF using *in-situ* solvothermal synthesis, ii) to examine the surface modification of AHF with coat seeding sol-gel zirconium nanoparticles prepared using sol-gel Pechini method prior to the growth of UiO-66 membrane and iii) to investigate the effectiveness of membrane samples prepared using single deposition UiO-66, second deposition of UiO-66 and UiO-66 deposited onto AHF modified by zirconium nanoparticles for the removal of HA. Four main phases involved in this study which are i) preparation of AHF using spinning based phase inversion and sintering technique, ii) deposition of UiO-66 membrane onto AHF using single and second deposition techniques under controlled parameters, iii) deposition of UiO-66 membrane onto AHF modified with zirconium nanoparticles prepared using sol-gel Pechini method and iv) HA removal studies using cross-flow filtration. The AHF, UiO-66 particles, and the developed UiO-66 membrane on AHF were characterized based on their physicochemical properties. All prepared samples were further tested for pure water flux test and HA removal test. For the single deposition technique, no UiO-66 membrane layer was observed where the UiO-66 solution was diffused within AHF's micropores. The UiO-66 membrane was successfully formed after the second deposition of UiO-66 and after coat-seeding with zirconium nanoparticles in the range of 1.5 μm to 11 μm thickness. The UiO-66 and zirconium particles acted as an anchor site for UiO-66 deposition by enhancing the adhesion and provided full coverage of the UiO-66 membrane onto AHF. It was found that the pure water fluxes for all prepared samples reduced ranging from 13.00 to 163.88 L m^{-1} h^{-1} as compared to pristine AHF's pure water flux of 259.67 L m^{-1} h^{-1}. These reductions of water flux were due to the presence of UiO-66 particles and zirconium nanoparticles on the entire surface of the AHF that increased the mass transfer resistance of water permeation across the membranes. Study on HA removal using UiO-66 membrane revealed that the prepared samples showed excellent performance of HA removal with 99 % rejection and satisfied solute fluxes ranging from 3.16 to 68.37 L m^{-1} h^{-1}. The high removal of HA can be explained by similar negative charge between UiO-66 particles and HA molecules which created charge repulsion between the surface of the membrane and the HA. This study concluded that UiO-66 membrane had been successfully deposited onto modified AHF with zirconium nanoparticles. Results from this study provided solutions on the difficulty of synthesizing well-developed, defect-free and well-continuous of UiO-66 membrane onto AHF with excellent HA rejection, moderate solute flux of UiO-66 membrane onto AHF.

ABSTRAK

Teknologi membran dengan menggunakan gentian gerongga alumina (AHF) yang dimendapkan dengan rangka logam organik (MOF) berasaskan zirkonium dikenali sebagai UiO-66 menawarkan pilihan terbaik untuk membuang asik humik (HA) yang wujud dalam sistem air. Kekangan utama perkembangan UiO-66 di atas AHF adalah kesukaran untuk membangunkan lapisan UiO-66 di atas AHF yang selanjar dan bebas kecacatan disebabkan mikroliang berlebihan dan bentuk tiubnya, menghasilkan kestabilan yang rendah dan penyingkiran HA yang lemah. Terdapat tiga objektif kajian ini iaitu i) mengkaji enapan tunggal serta enapan kedua membran UiO-66 di atas AHF menggunakan sintesis larutan haba *in-situ*, ii) memeriksa pengubahsuaian permukaan AHF dengan pembenihan salutan gel-larutan zarah nano zirkonium menggunakan kaedah gel-larutan Pechini sebelum pertumbuhan membran UiO-66 dan iii) menyelidik keberkesanan sampel membran yang disediakan oleh enapan tunggal UiO-66, enapan kedua UiO-66 dan enapan UiO-66 di atas AHF yang diubah suai dengan zarah nano zirkonium untuk penyingkiran AH. Empat fasa utama terlibat dalam kajian ini iaitu i) penyediaan AHF menggunakan pemintalan berasas fasa penyongsangan dan pensinteran, ii) pengenapan membran UiO-66 di atas AHF menggunakan teknik enapan tunggal dan kedua di bawah parameter kawalan, iii) enapan membran UiO-66 di atas AHF yang diubah suai dengan zarah nano zirkonium disediakan dengan kaedah gel-larutan Pechini dan iv) penyingkiran HA menggunakan penapisan aliran silang. AHF, zarah UiO-66 dan pembentukan membran UiO-66 di atas AHF telah dicirikan dalam pencirian terma fisikokimia. Kesemua sampel yang telah disediakan telah diuji dengan lanjut untuk ujian fluks air bersih dan ujian penyingkiran HA. Untuk teknik enapan tunggal, tiada lapisan membran UiO-66 diperhatikan di mana larutan UiO-66 telah meresap di antara mikroliang AHF. Membran UiO-66 telah berjaya dibentuk selepas enapan kedua membran UiO-66 dan selepas pembenihan salutan zarah nano zirkornium dengan julat ketebalan di antara 1.5 μm hingga 11 μm. Zarah UiO-66 dan zirkonium telah bertindak sebagai tapak penambat bagi enapan UiO-66 dengan meningkatkan keterlekatan dan memberi liputan penuh membran UiO-66 di atas AHF. Kajian ini mendapati bahawa fluks air bersih bagi semua sampel telah berkurang dalam julat 13.00 hingga 163.88 L m^{-1} h^{-1} berbanding fluks air bersih bagi AHF iaitu 259.67 L m^{-1} h^{-1}. Pengurangan fluks air bersih disebabkan oleh kehadiran zarah UiO-66 dan zarah nano zirkonium di atas keseluruhan permukaan AHF di mana meningkatkan rintangan pemindahan jisim penelapan air merentasi membran. Kajian terhadap penyingkiran HA mendedahkan bahawa sampel yang disediakan menunjukkan prestasi cemerlang penyingkiran HA dengan 99 % penyisihan dan fluks zat terlarut yang memuaskan dalam julat 3.16 hingga 68.37 L m^{-1} h^{-1}. Penyingkiran HA yang tinggi boleh dijelaskan dengan cas negatif yang sama di antara zarah UiO-66 dan molekul HA di mana berlakunya penolakan cas di antara permukaan membran dan HA. Kajian ini telah menyimpulkan bahawa membran UiO-66 telah berjaya dienapkan di atas AHF yang telah diubahsuai dengan zarah nano zirkonium. Hasil kajian ini menyediakan penyelesaian terhadap kesukaran pensintesisan membran UiO-66 di atas AHF terbaik yang bebas dari kecacatan dan selanjar dengan penyingkirann HA terbaik, fluks zat terlarut yang sederhana, dan bebas kecacatan.

TABLE OF CONTENTS

TITLE		PAGE
DECLARATION		**iii**
DEDICATION		**iv**
ACKNOWLEDGEMENT		**v**
ABSTRACT		**vi**
ABSTRAK		**vii**
TABLE OF CONTENTS		**viii**
LIST OF TABLES		**xii**
LIST OF FIGURES		**xiii**
LIST OF SYMBOLS		**xviii**
LIST OF ABBREVIATIONS		**xx**
LIST OF APPENDICES		**xxiii**
CHAPTER 1	**INTRODUCTION**	**1**
1.1	Research Background	1
1.2	Problem Statement	6
1.3	Objectives of Study	7
1.4	Scopes of Study	8
1.5	Research Contributions	10
1.6	Thesis Organization	10
CHAPTER 2	**LITERATURE REVIEW**	**13**
2.1	Background of Humic Acid	13
2.2	Humic Acid Removal using Membrane Filtration	14
2.3	Alumina Hollow Fiber as Support for UiO-66 Deposition	19
2.4	Metal-Organic Frameworks (MOFs)	25
	2.4.1 Background of MOFs	25
	2.4.2 Nucleation and Growth of MOFs	27

2.4.3 Adsorption Properties of Metal-Organic Framework 28

2.4.4 Zirconium based Metal-Organic Framework 30

2.4.5 Modulated Synthesis of High Crystallinity of UiO-66 43

2.5 Development In-Situ Growth UiO-66 on Alumina Hollow Fiber 46

2.5.1 Introduction Coat-Seeded Particles prior to UiO-66 Growth 54

2.5.2 Multi Deposition of MOFs 55

2.5.3 Modified Alumina Hollow Fiber with Zirconium Nanoparticles Prepared by Sol-gel Pechini Method 56

CHAPTER 3 RESEARCH METHODOLOGY 61

3.1 Introduction 61

3.2 Materials Selection 63

3.3 Development UiO-66 Membrane onto Alumina Hollow Fiber 63

3.3.1 Preparation of Asymmetric Alumina Hollow Fiber 63

3.3.2 Single-step Deposition of UiO-66 particles on Alumina Hollow Fiber 66

3.3.3 Second Deposition of UiO-66 Membrane 67

3.3.4 Deposition of UiO-66 onto Modified Alumina Hollow Fiber using Sol gel Pechini of Zirconium (ZrO_2) nanoparticles 67

3.4 Characterizations 70

3.4.1 Surface Roughness Analysis 70

3.4.2 Morphological Studies 70

3.4.3 Pore Size Distribution Analysis 71

3.4.4 Advanced Morphological Studies 71

3.4.5 Zirconium Element Analysis 71

3.4.6 Crystallinity Measurement 71

3.4.7 Effective Surface Area Analysis 72

3.4.8 UiO-66 Particle Functional Groups Detection 72

3.4.9 Mechanical Strength Measurement 72

3.4.10 Contact Angle Measurement 73

3.4.11 UiO-66 Particle Elements Detection 74

3.4.12 Surface Charge of UiO-66 Particle Analysis 74

3.4.13 Stability Test with Nitrogen Gas Purging 74

3.5 Performance Studies 75

3.5.1 Pure Water Flux Test 75

3.5.2 Humic Acid Removal Studies based Cross-flow Filtration 76

CHAPTER 4 RESULTS AND DISCUSSION 79

4.1 General Preview 79

4.2 Development of UiO-66 membrane on Asymmetric Alumina Hollow Fiber using In-situ Solvothermal Synthesis 80

4.2.1 Preparation of Asymmetric Alumina Hollow Fiber (AHF) using Phase Inversion and Sintering Technique 80

4.2.2 Preparation of UiO-66 Membrane onto Alumina Hollow Fiber 82

4.2.3 Humic Acid Removal using Single Deposition UiO-66 Particles deposited on Alumina Hollow Fiber 89

4.3 Deposition of UiO-66 Membrane onto Alumina Hollow Fiber using Second Deposition 95

4.3.1 In-situ Solvothermal Synthesis of UiO-66 membrane 95

4.3.2 Development of UiO-66 Membrane onto Alumina Hollow Fiber 100

4.3.3 Humic Acid Removal using Second Deposition of UiO-66 Membrane on Alumina Hollow Fiber 104

4.4 Modification of Alumina Hollow Fiber with Sol-Gel Pechini of Zirconium Nanoparticles as a Coat-Seeded Layer 107

4.4.1 Preparation of Zirconium Nanoparticles using Sol-gel Pechini Method 108

4.4.2 Development UiO-66 Membrane onto Modified Alumina Hollow Fiber 111

4.4.3 Humic Acid Removal using Single Deposition UiO-66 Membrane deposited on Modified Alumina Hollow Fiber with Zirconium Nanoparticles 116

CHAPTER 5 CONCLUSION AND RECOMMENDATIONS 123

5.1 Conclusions 123

5.2 Recommendations 126

REFERENCES 129

APPENDICES 145

LIST OF PUBLICATIONS 161

LIST OF TABLES

TABLE NO.	TITLE	PAGE
Table 2.1	NOM fractions and chemical group	14
Table 2.2	Methods of NOM removal	15
Table 2.3	Recent studies of HA removal using membrane filtration membrane	17
Table 2.4	Deposition of porous materials onto ceramic hollow fiber	22
Table 2.5	Crystal structures of five new zirconium MOFs	33
Table 2.6	BET surface area of synthesis UiO-66	42
Table 2.7	Recent studies of the growth of MOF on the support membrane for different applications	52
Table 2.8	Particle size of crystal zirconium nanoparticles	60
Table 3.1	The details of the experimental procedure	65
Table 3.2	Sample designs upon different synthesis's condition	69
Table 4.1	Properties list of AHF.	82
Table 4.2	Mass of MOF UiO-66 before and after the solvothermal synthesis	83
Table 4.3	BET surface area of UiO-66 particles prepared using the solvothermal synthesis	87
Table 4.4	The different mass loading of UiO-66 for second deposition growth of UiO-66	95
Table 4.5	Summary of BET results	98
Table 4.6	Contact angle analysis	103
Table 4.7	The crystallite size of zirconium nanoparticles.	110
Table 4.8	Mass Loading of UiO-66 deposited onto modified AHF	111
Table 4.9	Summary data on performance studies for all design samples	120
Table 4.10	Comparison of humic acid removal studies for different membrane types	121

LIST OF FIGURES

FIGURE NO.	TITLE	PAGE
Figure 1.1	Molecular structure of humic acid	1
Figure 1.2	Zirconium metal cluster to form a UiO-66 framework	4
Figure 2.1	Schematic diagram of adsorption mechanism toward HA	18
Figure 2.2	Schematic diagram of asymmetric alumina hollow fiber membrane	20
Figure 2.3	Step by step procedures of spinning based phase inversion and sintering technique	21
Figure 2.4	FESEM images of zeolite growth on the alumina hollow fiber at 1500 magnifications	24
Figure 2.5	Schematic diagram of MOF	26
Figure 2.6	Example of MOFs structure	26
Figure 2.7	a) Different synthesis routes of MOF preparation and b) Summary of common synthesis route	27
Figure 2.8	Solvothermal synthesis of MOFs	28
Figure 2.9	a) Illustration of adsorption using MOF b) Various adsorption mechanisms promoting by MOFs	29
Figure 2.10	Simulated lattice parameter as a function of water content	30
Figure 2.11	Articles reporting UiO-66 as a subject area in Web of Science database (Year 2009 till 2018)	31
Figure 2.12	Crystal structure of UiO-66 which occupied with two different balls from a top view (Yellow ball is 8 Å open pore and Pink ball is 6 Å open pore)	32
Figure 2.13	A common types of zirconium-based MOF series	32
Figure 2.14	PXRD patterns of different UiO-66 substitutes	36
Figure 2.15	Imidazolate bonding with metal ions relatively to Si-O-Si	37
Figure 2.16	XRD results of UiO-66 powders as prepared and after stability test	38
Figure 2.17	XRD results upon thermal treatment	38
Figure 2.18	Nitrogen adsorption-desorption isotherm	40

Figure 2.19	Types of hysteresis loop	41
Figure 2.20	Illustration of well-defined flipping of benzene ring resulting different open-pore entrance sizes	43
Figure 2.21	The effect of modulator attributed the Zr-based metal-organic framework's properties. a) Morphology, b) Stability, c) Defect concentration, d) Effective surface area, S_{BET}, e) Pore size entrance and d) Stability vs defect concentration	45
Figure 2.22	a) The potential outcomes of modulators utilization, b) Top view of defect-free UiO-66, c) Defective structure of UiO-66 by missing linker and d) Defective structure of UiO-66 by missing metal cluster	46
Figure 2.23	A schematic diagram of in-situ solvothermal synthesis of UiO-66 onto ceramic substrate	48
Figure 2.24	SEM images of the development UiO-66 onto porous YSZ substrate. a-b) 2 hours, c-d) 4 hour, e-f) 12 hours, g-h) 24 hours and i-j) 48 hours	48
Figure 2.25	a) Schematic diagram of Zr species occupied micro channel, b) SEM image the polycrystalline layer of UiO-66 and c) EDX mapping Al and Zr species	49
Figure 2.26	Development of UiO-66 on the YSZ micropatterned substrate. a) Casting technique on the YSZ micropatterned substrate, b) Final product of YSZ micropatterned substrate and c) the 3D optical images of the YSZ micropatterned substrate	50
Figure 2.27	Water permeability (left) and salt rejection (right) of the design UiO-66 membrane according to different case studies of the defect-free, missing linker, and missing cluster	51
Figure 2.28	FESEM image of defect UiO-66 membrane. a) Delamination of UiO-66 membrane when immersed in distill water and an hour sonication and b) Peel-off UiO-66 membrane when immersed in 10 % HCl aqueous solution and an hour sonication	54
Figure 2.29	Schematic diagram of preparation MIL-53 on alumina substrate	56
Figure 2.30	Scanning electron microscopy (SEM) images. a) top view and b) cross-section view	56
Figure 2.31	Step procedures of ZIF membrane preparation	57
Figure 2.32	UiO-66 membrane development including sol-gel coating of zirconium crystal particles	57

Figure 2.33	Different routes of sol-gel preparation	58
Figure 2.34	FESEM image of zirconium	59
Figure 2.35	XRD of crystal zirconium nanoparticles a) 650 °C, b) 540 °C and c) 490 °C	60
Figure 3.1	Research design of experimental procedures	62
Figure 3.2	Spinning based phase inversion experimental setup	64
Figure 3.3	Sintering profile of AHF	65
Figure 3.4	In-situ solvothermal synthesis of UiO-66 onto alumina hollow fiber	66
Figure 3.5	Schematic diagram of experimental procedure	68
Figure 3.6	Schematic diagram of three-point bending apparatus	73
Figure 3.7	Schematic diagram of N_2 purging system for water stability test	75
Figure 3.8	Schematic diagram of dead-end filtration setup for HA removal studies	77
Figure 4.1	FESEM images of AHF membrane prepared using spinning-based phase inversion. a) Overall cross-section image at 200 μm magnification, b) Wall thickness cross section image at 50 μm magnification, c) AFM image of surface roughness of AHF and d) Mercury porosimetry analysis for pore size distribution data	81
Figure 4.2	FESEM/EDX images of MOF UiO-66 on AHF membranes prepared for 24 hours using various concentrations of precursors. i) FESEM images of the ceramic membrane deposited with MOF and ii) EDX mapping for zirconium	84
Figure 4.3	FESEM/EDX images of MOF UiO-66 on AHF membranes prepared for 120 hours using various concentrations of precursors. i) FESEM images of ceramic support deposited with MOF and ii) EDX mapping for zirconium.	85
Figure 4.4	X-ray diffraction peaks for UiO-66 particles. The signature peaks representing UiO-66 were represented with *. a) Synthesis period of 24 hours and b) synthesis period of 120 hours.	86
Figure 4.5	N_2 adsorption isotherms for UiO-66 particles.	87
Figure 4.6	Mercury porosimetry analysis for AHF supports before and after the deposition of MOF UiO-66. a) 24 hours synthesis period and b) 120 hours synthesis period.	88

Figure 4.7 Pure water flux for pristine AHF and the membrane deposited with UiO-66 particles, prepared using various synthesis conditions 89

Figure 4.8 Solute fluxes of pristine AHF membrane and the ceramic membranes deposited with UiO-66 and humic acid rejection 90

Figure 4.9 Feed and permeation samples taken during the filtration processes. a) Feed with 1000 mg L^{-1} humic acid and filtration samples at the permeate stream after b) 10 minutes, c) 20 minutes, d) 30 minutes, e) 40 minutes, f) 50 minutes and g) 60 minutes using M3 samples 91

Figure 4.10 Zeta potential analysis of UiO-66 particles and HA molecules 92

Figure 4.11 Stability results for membrane samples a) M1, b) M3, c) M5 and d) M7. N_2 permeance before (●) and after (■) the membrane samples immersed in boiling water overnight. 94

Figure 4.12 FESEM images of UiO-66 particles. a) M3 and b) M11 97

Figure 4.13 Nitrogen adsorption-desorption based BET analysis 98

Figure 4.14 XRD result of UiO-66 powders in compared with AHF powder 99

Figure 4.15 FTIR-ATR spectrum 100

Figure 4.16 FESEM/EDX images for-66 for different Zr concentrations and time synthesis of 24 hours. i) SEM images of surface alumina support growth with UiO-66, ii) Cross-section SEM images, iii) EDX mapping of Al (yellow color) and Zr (purple color) 101

Figure 4.17 FESEM/EDX images for UiO-66 for second growth with different time synthesis. i) SEM images for surface alumina growth with UiO-66, ii) SEM images of cross-section and iii) EDX mapping of Al (yellow color) and Zr (purple color). 102

Figure 4.18 Pure water flux of all prepared samples for single and dual deposition 105

Figure 4.19 Humic acid performance test (■) Humic acid permeation and (●) Humic acid rejection 106

Figure 4.20 Treated samples after the filtration process for humic acid removal with concentration feed of 1000 mg L^{-1} within 1 hour 107

Figure 4.21	FESEM images of AHF modified with zirconium nanoparticles. a) FESEM image of pristine AHF, b) AHF after been growth with zirconium nanoparticles prepared using sol-gel Pechini method and c) FESEM image of zirconium nanoparticles at magnification of 100 K.	108
Figure 4.22	XRD pattern of zirconium nanoparticle	109
Figure 4.23	Adsorption desorption equilibrium of nitrogen adsorption	110
Figure 4.24	FESEM images for a) M3, b) M11, c) M15 and d) M16. i) FESEM images of the cross-section area of UiO-66 on the AHF and ii) FESEM images of the top surface of UiO-66 on AHF	112
Figure 4.25	Schematic diagram of development UiO-66 onto AHF coated zirconium nanoparticles. a) UiO-66 in-situ growth on AHF with zirconium nanoparticles, b) metal cluster of UiO-66, and c) Interactions exist between AHF and zirconium nanoparticles, UiO-66 and zirconium nanoparticles via hydrogen bond	113
Figure 4.26	AFM analyses and contact angle. a) AHF modified with zirconium nanoparticles prepared using sol-gel Pechini method and b) AHF growth with zirconium nanoparticles and UiO-66 membrane	114
Figure 4.27	XPS spectra of UiO-66 particles of 0.1 M of zirconium chloride concentration	115
Figure 4.28	a) Pure water flux test and b) HA for all prepared samples consisting of UiO-66 deposited on modified AHF with zirconium nanoparticles	117
Figure 4.29	Development of UiO-66 onto modified AHF with coat seeded zirconium nanoparticles and its mechanism of HA removal	118
Figure 4.30	a) Zeta potential analysis of UiO-66 particles prepared by different Zirconium chloride concentrations and b) Isoelectric point of different materials. (■) UiO-66 particles prepared using zirconium chloride concentration of 0.034 M (M3) and (●) UiO-66 particles prepared using zirconium chloride concentration of 0.1 M (M11).	119

LIST OF SYMBOLS

δ^-	-	Electronegative
%	-	Percentage
*	-	Asteric symbol
δ^+	-	Electropositive
Δm_{feed}	-	Weight difference of feed solution
ΔP	-	Pressure gradient
Δt	-	Time interval
°	-	Degree
°C	-	Degree celcius
µm	-	Micrometer
A	-	Total surface area
A_i	-	Final concentration of humic acid solution at feed
A_m	-	Area of the permeation cell
Ao	-	Initial concentration of humic acid solution at permeate
C_{ff}	-	Final concentration of the feed
C_{id}	-	Initial concentration of the sweep liquid
cm	-	Sentimeter
Dhkl	-	Size along (hkl) direction
D_i	-	Inside diameter
D_o	-	Outside diameter
eV	-	Electron volt
F	-	Maximum load
g	-	Gram
h	-	Hours
H_i	-	HA final mass
H_o	-	HA initial mass
J	-	Gas flux of nitrogen
J_v	-	Solute flux
J_W	-	Pure water flux
K	-	Scherer constant (0.89)

L	-	Length of AHF
L	-	Liter
m	-	Meter
M	-	Molar
$m^2 g^{-1}$	-	Per meter square per gram
$mg\ g^{-1}$	-	Milligram per gram
$mg\ L^{-1}$	-	Milligram per Liter
mm	-	Milimeter
MPa	-	Mega pascal
nm	-	Nanometer
Pa	-	Pascal
ppm	-	Part per million
Q	-	Total nitrogen flow rate
S_{BET}	-	Effective surface area (BET analysis)
t	-	Time
W	-	Watt
α	-	Alpha
β	-	Full- width at half-maximum
θ	-	Diffraction angle
λ	-	X-ray wavelength
Π	-	Pi
ρ_{feed}	-	Density of feed solution
σF	-	Fracture strength

LIST OF ABBREVIATIONS

3D	-	Three dimension
AFM	-	Atomic field microscopy
AHF	-	Alumina Hollow Fiber
Al/Al_2O_3	-	Alumina
ALD	-	Atomic layer deposition
AOP	-	Advanced oxidation process
APTES	-	Aminopropyltriethoxysilane
AR	-	Analytical reagent
ATR	-	Attenuated total reflection
BDC	-	Benzene dicarboxylic
BET	-	Brunauer-Emmet-Teller
BPDC	-	Biphenyl-dicarboxylic acid
BSA	-	Bovine serum albumin
BTC	-	Benzene- tricarboxylic acid
BTEX	-	Benzene, Toluene, Ethylbenzene and Xylene
CAU	-	Christian-Albrecht-University
CCP	-	Cubic close packed
CMS	-	Carbon molecular sieve
COOH	-	Carboxyl
Cr	-	Chromium
CVD	-	Chemical vapor deposition
DMF	-	Dimethyl formamide
EDX	-	Energy dispersive X-Ray
EG	-	Ethylene glycol
ELP	-	Electroless plating
FA	-	Fulvic acid
FESEM	-	Field emission scanning electron microscopy
FTIR	-	Fourier-transform infrared spectroscopy
FWHM	-	Full width at half maximum
GO	-	Graphene oxide

GPU	-	Gas permeance unit
HA	-	Humic acid
HAA	-	Haloacetic acids
HCl	-	Hydrocloric acid
HKUST	-	Hong Kong University of Science and Technology
Hmim	-	2-methylimidazole
HS	-	Humic substances
ID	-	Inside diameter
IR	-	Isoreticular
JCPDS	-	Join Committee on Powder Diffraction Standard
LSCF	-	Lanthanum strontium cobalt ferrite
LMH	-	Liter per meter square per hour
M	-	Monoclinic
MIL	-	Material Institute Loisivier
MIP	-	Mercury intrusion porosimetry
MMM	-	Mixed matrix membrane
MOF	-	Metal organic framework
MTB	-	Methanetetrayltetrabenzoic acid
MTBE	-	Methanol/methyl tert-butyl ether
MW	-	Molecular weight
NA	-	Not available
NDC	-	Naphthalene dicarbocyclic
NF	-	Nanofiltration
NH	-	Amino
NMR	-	Nuclear magnetic resonance
NMP	-	N-methyl pyridione
NOM	-	Natural organic matter
OD	-	Outside diameter
PAN	-	Polyacrylonitrile
PEG	-	Polyethylene glycol
PEI	-	Polyethylenimine
PES	-	Polyethersulfone
PESf	-	Polyethersulfone
PIM	-	Polymer intrinsic microscopy

PS	-	Post-synthesis
PSM	-	Post-synthetic modification
PTFE	-	Polytetrafluoroethylene
PVDF	-	Polyvinylidene fluoride
PVP	-	Polyvinylpryridione
PXRD	-	Powder X-ray diffraction
PZDC	-	Pyrazole-3,5-dicarboxylic acid
QENS	-	Quasi-elastic neutron scattering
S	-	Sample
SBU	-	Secondary building unit
SEM	-	Scanning electron microscopy
SiC	-	Silanization
SiO_2	-	Silica oxide
SOFC	-	Solid oxide fuel cells
T	-	Tetragonal
TEM	-	Transmission electron microscopy
TEOS	-	Tetraethylorthosilicate
TFBDC	-	Tetrafluoro-1,4-benzenedicarboxylic acid
THM	-	Trihalomethane
TiO_2	-	Titanium oxide
TMP	-	Trans membrane pressure
TPDC	-	Terphenyl-dicarboxylate acid
UiO	-	University of Oslo
UV	-	Ultra violet
UV-VIS	-	Ultra violet-visible
XPS	-	X-ray photo spectroscopy
XRD	-	X-ray diffraction
YSZ	-	Yttria-stabilized zirconium
ZIF	-	Zeolitic imadazolate framework
ZnO	-	Zinc oxide
Zr	-	Zirconium
ZrO_2	-	Zirconium

LIST OF APPENDICES

APPENDIX	TITLE	PAGE
Appendix A	Molecular Structure Of Selected Materials	145
Appendix B	Molecular Structure Of Selected Materials	147
Appendix C	Mercury Porosimetry of AHF	149
Appendix D	Nitrogen Stability Test	151
Appendix E	Performance Test Raw Data (Single Deposition UiO-66 onto AHF)	153
Appendix F	Performance Test Raw Data (Second Deposition UiO-66 onto AHF	156
Appendix G	Performance Test Raw Data (Deposition UiO-66 onto modified AHF	158
Appendix H	Adsorption-desorption Equilibrium	160

CHAPTER 1

INTRODUCTION

1.1 Research Background

Humic acid (HA) is a natural organic matter (NOM) that naturally presents in raw water sources (i.e. lakes, rivers, and streams) as a result of the decomposition of dead animals and plants. HA has a complex structure with three functional groups, namely, carboxylic acids, phenolic alcohols and methoxyl carbonyls as shown in Figure 1.1. Typically, HA can be detected through its brownish appearance at concentrations above 5 mg L^{-1} [1]. According to the World Health Organization (WHO), the allowance content of HA in drinking water should not exceed 100 µg L^{-1} [2]. However, conventional treatment of wastewater through chlorination causes HA to react with chlorine, generating trihalomethane (THM) and haloacetic acids (HAA), which are known as human carcinogens [1–3]. Thus, it is crucial to remove any HA prior to conventional chlorination of drinking water. One way to achieve this is through membrane technology.

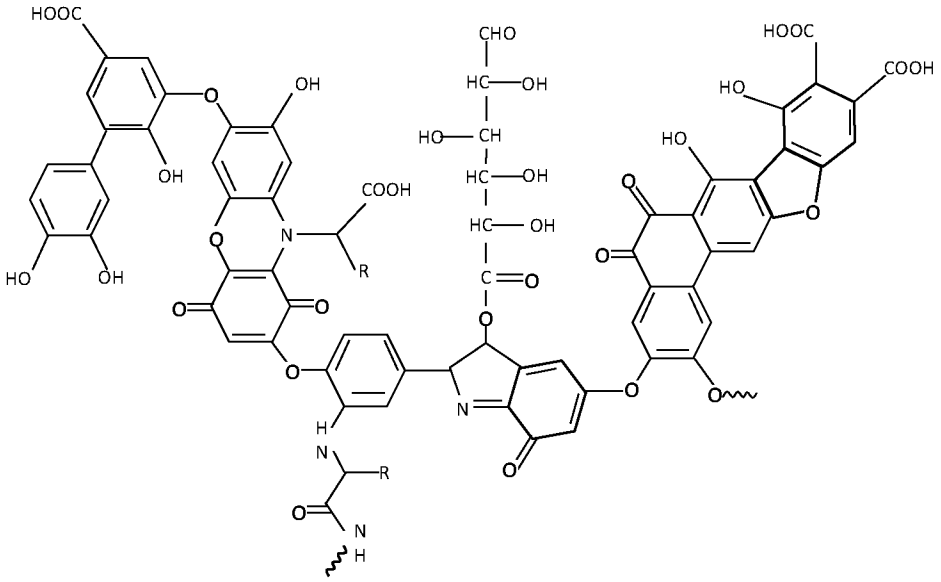

Figure 1.1 Molecular structure of humic acid [4]

Typically, polymer materials are preferable for membrane preparation as ascribed by their easy availability, simple preparation process, and excellent performance. However, ceramic membranes have recently received significant attention in water treatment, specifically in water purification. The emerging use of ceramic membranes are ascribed by their higher chemical stability, excellent mechanical strength, and good thermal stability. Besides that, ceramic membranes can be tailored to have unique morphologies, consisting of finger-like and sponge-like structures [5,6]. Unlike gas separation application that requires thin and dense structures for excellent selectivity and permeability [7,8], liquid separation using ceramic membranes can occur over the entire porous ceramic membrane [9]. This unique structure can be fabricated easily during the membranes' initial preparation stage. The preparation of ceramic membranes can be done by using phase inversion and sintering techniques [10–13]. Three main steps are involved in this process, namely a) preparation of a ceramic suspension, b) phase inversion process of ceramic suspension, and c) sintering process of the membrane precursor [14,15]. In the preparation of the ceramic suspension, ceramic particles with different particle sizes are mixed with a polymer binder, an organic solvent, and an additive using a planetary ball mill to obtain a homogenous ceramic suspension.

To obtain ceramic membranes with hollow fiber configuration, the ceramic suspension is extruded through a spinneret with water as an internal coagulant to create the lumen. The suspension is then further extruded into a water coagulation bath to solidify the polymer and freeze the ceramic particles. However, this process is generally affected by various parameters, i.e. extrusion rate, bore fluid rate, air gap, type of internal coagulant/external coagulant, and temperature of internal coagulant/external coagulant. Thus, to obtain pure ceramic membranes, the membrane precursor has to be sintered at a temperature ranging from 1300 – 1700 °C. In this process, grain boundaries are growing, providing dense structures and contributing to high mechanical strength. Although ceramic membranes can be used directly in water separation processes, it is limited only to the ultrafiltration range, as reported in previous studies [11,12]

To overcome this limitation, ceramic membranes need to be incorporated with microporous/mesoporous materials for HA removal from wastewater. In this context, ceramic membranes act as porous support in which novel micro/mesoporous materials are deposited using various conventional coating techniques (i.e. paintbrush, spray and dip coating) [16,17], electroless plating [18,19], and hydrothermal/solvothermal growth [20–22]. Many porous materials have been incorporated on ceramic membranes to improve the separation performance of ceramic membranes, i.e. zeolite, graphene oxide, metal-organic framework (MOF), and metal oxides. Among these materials, MOF has received much attention to be incorporated on ceramic membranes. There are approximately 20, 000 MOFs that have been discovered by various researchers such as Material Institute Loisivier (MIL), UiO-66, UiO-67, UiO-68 (which UiO is referring to University of Oslo), Hong Kong University of Science and Technology (HKUST), isoreticular MOF (IR-MOF), and zeolitic imidazolate framework (ZIF). Each of the MOF materials is distinguished by different ligands and metals. These highly porous materials with crystalline structures bonded by organic ligands connected to metal ions and carboxylate ions [23]. MOFs have a unique chemical versatility with a tailored framework relative to zeolite, thus they can act as promising materials that can accommodate guest molecules [24].

To use MOF for water purification/separation applications, remarkable water stability is crucial criteria, apart from their crystallinity and porosity. Most MOFs are unstable in water, and their structure would be destructed as water molecules can attack and eventually cause ligand displacement and structural decomposition of the synthesized MOFs [25]. Among all the MOFs material, zirconium (Zr) based MOF known as a UiO-66 (referring to University of Oslo) possesses all of the characteristics required for water purification application such as superior water stability, high hydrothermal stability under acidic and basic conditions, and the ability to separate small particles in the range of ~6 Å [20,22]. UiO-66 is constructed by high valence metal of Zr^{4+} that has high charge density that can create stronger coordination with organic ligand attributed to Coulombic interaction of the highly oxophilic Zr^{4+} metal sites with the negatively charged termini of the carboxylate linkers [25,26].

Besides, UiO-66 has carboxyl groups that enhance the surface hydrophilicity and increase the performance of water purification treatment, particularly HA removal. Figure 1.2 shows the zirconium metal cluster connected by carboxylate linkers to develop the unique molecular structure of UiO-66. Recent interest in these materials is mostly focused on synthesis routes, i.e to extend the pore size, increase the surface area, and enhance the structural stability of the respective materials. In order to predict the capability of MOFs, it is vital to study the construction of the MOF building units. MOFs should display strong bonding providing robustness, linking units that are available or modification by organic synthesis and a geometrically well-defined structure [27,28]. In general, MOFs can be synthesized by different processes, such as conventional synthesis, electrochemistry, microwave-assisted heating, mechanochemistry, and sonochemistry process [23,29]. The conventional synthesis includes solvothermal and non-solvothermal synthesis or known as hydrothermal synthesis. The solvothermal synthesis is the most commonly for synthesizing MOFs ascribed by its simplicity, large-scale growth of crystals with high levels of crystallinity, phase purity, and surface areas [30].

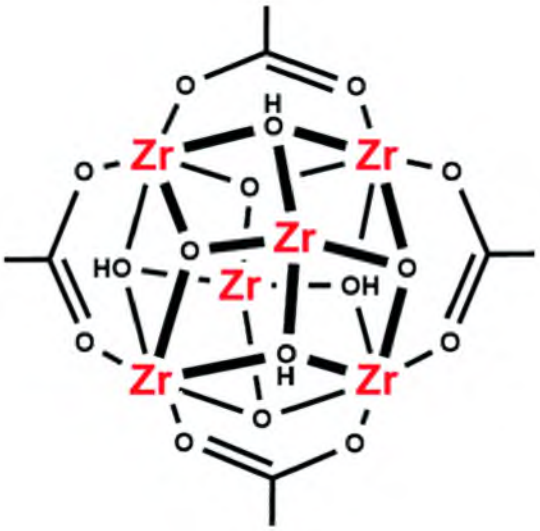

Figure 1.2 Zirconium metal cluster to form a UiO-66 framework [27]

MOFs also have been used as membranes for various separation processes. The easiest way to use MOFs as membrane' material is by developing a mixed matrix membrane (MMM) that uses MOFs as an inorganic filler [31]. However, MMM has a drawback whereby the inorganic filler aggregation and compatibility between the inorganic filler and polymers always remain a major issue [32,33]. Therefore, another

alternative is by growing MOF on a support membrane to solve the issue related to aggregation and incompatibility. Various studies have reported the successful growth of MOF on an inert support, i.e. HKUST (referring to The Hong Kong University of Science and Technology) [34–36], MIL (referring to Materials of Institute Lavoisier) [37,38], and ZIF-8 (referring to zeolitic imidazolate framework) [39–42]. However, ceramic support especially alumina hollow fiber (AHF), offered the best option for *in-situ* growth of MOF rather than polymer support membrane. The main reason is the presence of abundant hydroxyl group (OH^-) on the surface of AHF act as an anchor point for any surface assemblies and well continuity and development of a free-defect layer of MOF [19,43]. For the case of Zr-based MOFs, several research works have successfully prepared UiO-66 deposited onto AHF for various applications, i.e. desalination [20,44], arsenic removal [21], organic removal [45], and gas application [22,46].

In order to develop a well continuous UiO-66 membrane on the AHF particularly in tubular configuration, the UiO-66 synthesis conditions i.e metal loading (zirconium chloride concentration), synthesis period, and numbers of UiO-66 deposition on AHF play such vital role. The advancement of the development of UiO-66 membrane on AHF resulted in its potential in a wide range of applications as aforementioned and useful to remove HA that naturally present in water sources. Membrane technology can be regarded as a promising alternative to remove HA due to its simple removal mechanism which is adsorption and filtration. Besides, the deposition UiO-66 on AHF resulted to abundant negative charged of carboxyl groups ($COOH^{-1}$) that can create charge repulsion effect with negatively charged carboxyl groups belong to HA molecules. Thus, it also aids to minimize the fouling formation due to the adsorption of HA molecules on the active surface of the design membrane in this study after contact time.

1.2 Problem Statement

Naturally, HA has strong adhesion on the surface of the hydrophobic membrane causing the poor performance of flux and selectivity. Thus, this study is focusing on the deposition of UiO-66 membrane onto alumina hollow fiber (AHF). To the best of our knowledge, there are no reported studies on HA removal using AHF deposited with UiO-66 membrane. Therefore, this study provides in-sight knowledge and understanding regarding HA removal using these materials. There are some limitations of using AHF as the porous support. AHF can hinder the well-developed, defect-free, and continuous intergrown of UiO-66 membrane on AHF due to its abundant micropores and tubular configuration. Apart from that, low nucleation of UiO-66 membrane and weak adhesion between UiO-66 and AHF's surface, hence, can cause UiO-66 membrane to delaminate [22]. This unfavorable deposition of the UiO-66 membrane can yield a low HA rejection in the membrane-based separation process.

In this study, the solvothermal synthesis conditions were studied through single deposition of UiO-66 onto AHF. Two different parameters were investigated which were synthesis periods and metal loading, which play vital role in developed UiO-66 membrane onto AHF. To develop a well and defect-free continuous UiO-66 membrane and enhance the adhesion between AHF and UiO-66 onto AHF, the surface modification of AHF by introducing a second deposition of UiO-66 membrane was studied. The second deposition of the UiO-66 membrane was introduced on the first deposition of UiO-66 that acts as a coat-seeded layer. This method has been demonstrated to be a viable technique to obtain a high UiO-66 membrane coverage on AHF. The abundant carboxyl groups ($COOH^{-1}$) of UiO-66 as a seeding crystal can functionalize the AHF's surface and promote UiO-66 crystallization. It also acts as the active and anchoring site by enhancing adhesion between the UiO-66 membrane and AHF.

In addition, this study was conducted by modifying AHF's surface with zirconium nanoparticles which were useful to improve the micro-defect at the surface of AHF. Zirconium nanoparticles were prepared using sol-gel Pechini method which is a common synthesizing route of synthesized metal oxide nanoparticles. Zirconium

nanoparticles were used as the coat-seeded particles considering the similarity of Zr-Zr species between UiO-66 and zirconium nanoparticles on AHF's surface, and thus can enhance the adhesion between UiO-66 membrane and AHF. Therefore, a stronger binding can be provided via the chemical bond between the surface AHF, coat-seeded particles of zirconium, and UiO-66 linker which are carboxylate groups, respectively. There are abundant hydroxyl groups (OH^{-1}) promoted by zirconium nanoparticles creating a hydrogen bond between the zirconium and UiO-66 via carboxylate linkers, hence, increase the adhesion between AHF and UiO-66 membrane.

1.3 Objectives of Study

This study aimed to prepare and characterize the UiO-66 membrane deposited on modified alumina hollow fiber (AHF) for HA removal. The objectives of the study are:

1. To study the single deposition and second deposition of UiO-66 membrane onto AHF using in-situ solvothermal synthesis at a constant 120 °C under different zirconium chloride concentrations and synthesis periods.
2. To examine surface modification of AHF with coat seeding sol-gel zirconium nanoparticles prepared using sol-gel Pechini method prior to the growth of UiO-66 membrane.
3. To investigate the effectiveness of HA removal for all prepared samples using single deposition UiO-66, second deposition of UiO-66 and UiO-66 deposited onto AHF modified by zirconium nanoparticles.

1.4 Scopes of Study

In order to achieve the aforementioned objectives, the scopes of study have been identified:

Scopes of Objective 1:

a) Fabricating AHF using spinning-based phase inversion and sintering technique for different conditions controlled i.e ceramic composition formula, extrusion rate, bore fluid rate, air gap, sintering temperature, and heating rate.

b) Characterizing AHF using scanning electron microscopy (SEM), atomic field microscopy (AFM), mercury intrusion porosimetry (MIP), mechanical strength, and pure water permeation test.

c) Preparing the UiO-66 mother solution for different zirconium chloride concentrations of 0.021 M, 0.034 M, 0.049 M and 0.051 M at constant zirconium chloride : BDC mass ratio is 1.4 [20].

d) Synthesizing UiO-66 membrane onto AHF using in-situ solvothermal synthesis for the constant solvothermal temperature at 120 °C under various synthesis period (24 hours and 120 hours)

e) Characterizing all design samples using field emission scanning electron microscopy (FESEM), energy dispersive X-Ray (EDX), X-ray diffraction (XRD), Brunauer-Emmet-Teller (BET), MIP, water stability test, and zeta potential analysis.

f) Preparing the UiO-66 mother solution for different zirconium chloride concentrations of 0.034 M and 0.1 M which selection was made according to Scopes (d) and (e).

g) Synthesizing in-situ solvothermal UiO-66 onto AHF with zirconium chloride concentrations of 0.034 M and 0.1 M at 120 °C of 24 hours.

h) Synthesizing the UiO-66 secondary deposition with zirconium chloride concentrations of 0.1 M at 120 °C for different synthesis periods of 24 hours, 48 hours, and 60 hours.

i) Conducting a series of characterization to examine physicochemical properties of design samples include FESEM, EDX, contact angle measurement, XRD, FTIR, and BET.

Scopes of Objective 2:

a) Preparing the sol-gel Pechini solution by mixing metal salt of zirconyl nitrate hydrate ($ZrO(NO_3)_2.xH_2O$), chelating agent (citric acid), cross-linking agent (ethylene glycol), and water.

b) Conducting polymerization proses of the sol-gel Pechini method at a calcination temperature of 400 °C for an hour.

c) Characterizing zirconium nanoparticle properties by using SEM, XRD, and BET analyses.

d) Preparing the UiO-66 mother solution for different zirconium chloride concentrations of 0.034 M and 0.1 M which selection was made according to Objective 1.

e) Synthesizing the in-situ solvothermal of UiO-66 onto AHF at the constant solvothermal temperature of 120 °C for 24 hours.

f) Examining the design samples properties using FESEM, AFM, and contact angle measurement.

Scopes of Objective 3:

a) Conducting a zeta potential test to examine the surface charge of UiO-66 particles.

b) Preparing an aqueous solution of HA with an initial concentration of 1000 mg L^{-1}. This concentration was selected as a maximum concentration of HA presence in the water system that can change due to topography, season, flood, drought, and human activities [47,48].

c) Conducting a compaction/stability for 30 minutes prior to pure water flux/ HA removal study.

d) Performing pure water flux test and HA removal for initial concentration of 1000 mg L^{-1} for the constant transmembrane pressure (ΔP) of 2 bar using cross-flow filtration for all prepared samples, respectively.

1.5 Research Contributions

This study is beneficial to the researchers in which provide more in-depth insights in the term of the preparation and characterization of metal-organic framework (MOF) of UiO-66 membrane deposited onto AHF using in-situ solvothermal synthesis. In addition to that, fundamental information of unique UiO-66 as an advanced class of porous materials can be further discussed that contribute knowledge on the development of other versatile nanomaterials. The design samples prepared in this study can solve the main challenge of unfavorable continuous MOF materials development on the hollow shape of substrate membrane, filling the gap of knowledge and beneficial to the scientific community to expand knowledge on versatile UiO-66 features for the water purification process. Finally, this area of study can be further commercialized based on UiO-66 membrane for water purification will convincingly depict the advantages of this MOF's material as an alternative solution for fouling issues in membrane technology.

1.6 Thesis Organization

This thesis starts with Chapter 1 that contains the research background of the HA, membrane materials, and metal-organic framework of UiO-66. This chapter also elaborates in detail of problem statement, objectives, and scope of studies. Next is Chapter 2 that has insight knowledge of the studies from the introduction of HA, ceramic membrane fabrication and surface modification, the background of metal-organic framework and UiO-66 itself, related studies on the UiO-66 developed on AHF for different applications.

In Chapter 3, there were four activities involved, which were 1) deposition UiO-66 onto AHF using in-situ solvothermal synthesis, 2) surface of AHF was modified with coat-seeded of UiO-66 particles prior to UiO-66 development known as a second deposition technique, 3) AHF was modified by coat-seeded of zirconium crystal nanoparticles prepared using sol-gel Pechini method prior to UiO-66 growth and 4) the performance tests of the design samples were tested based cross-flow filtration for HA removal.

Chapter 4 explains in detail the results gained from the experimental studies with insight discussion. In general, the UiO-66 layer was successfully developed on AHF after been modified by zirconium nanoparticles coat-seeded on the AHF's surface. The excellent rejection and permeation that was influenced by the charge repulsion effect between negatively charged carboxyl groups of UiO-66 and HA, respectively. Chapter 5 concluded the summary of this study. Some recommendations are suggested to improve this study for future works.

REFERENCES

1. Lowe. J., Hossain. M. M. Application of Ultrafiltration Membranes for Removal of Humic Acid from Drinking Water. *Desalination*, 2008. 218(1–3): 343–354.
2. Sudoh. R., Islam. M. S., Sazawa. K., Okazaki. T., Hata. N., Taguchi. S., et al. Removal of Dissolved Humic Acid from Water by Coagulation Method using Polyaluminum Chloride (PAC) with Calcium Carbonate as Neutralizer and Coagulant Aid. *J. Environ. Chem. Eng.*, 2015. 3(2): 770–774.
3. Levchuk. I., Rueda Márquez. J. J., Sillanpää. M. Removal of Natural Organic Matter (Nom) from Water by Ion Exchange – A Review. *Chemosphere.*, 2018. 192: 90–104.
4. Wo. A. Modified Polyphenol Binder Compositions and Methods For Making And using Same. US 20140094562 A1;1–26. 2016.
5. Kingsbury. B. F. K., Li. K. A Morphological Study of Ceramic Hollow Fibre Membranes. *J. Memb. Sci.*, 2009. 328(1–2):134–140.
6. Kingsbury. B. F. K., Wu. Z., Li. K. A Morphological Study of Ceramic Hollow Fibre Membranes: A Perspective on Multifunctional Catalytic Membrane Reactors. *Catal. Today.*, 2010. 156: 306–315.
7. Tan. X., Liu. Y., Li. K. Preparation of LSCF Ceramic Hollow-Fiber Membranes for Oxygen Production by a Phase-Inversion / Sintering Technique. *J. Am.. Cer. Soc.*, 2005. 44(1): 61–66.
8. Tan. X., Pang. Z., Li. K. Oxygen Production using $La_{0.6}Sr_{0.4}Co_{0.2}Fe_{0.8}O_{3-\delta}$ (LSCF) Perovskite Hollow Fibre Membrane Modules. *J. Memb. Sci.*, 2008. 310(1-2): 550–556.
9. Lee. M., Wu. Z., Wang. R., Li. K. Micro-structured Alumina Hollow Fibre Membranes – Potential Applications in Wastewater Treatment. *J. Memb. Sci.*, 2014. 461: 39–48.
10. Abdullah. N., Rahman. M. A, Ismail. A. F., Othman. M. H. D, Jaafar. J. Preparation of Ceramic Hollow Fiber Membrane Using Phase Inversion and Sintering Technique. *Adv. Materials.*, 2016. 1133: 141–145.

11. Abdullah. N., Rahman. M. A., Othman. M. H. D., Ismail. A. F., Jaafar. J., Aziz. A. A. Preparation and characterization of self-cleaning Alumina Hollow Fiber Membrane using the Phase Inversion and Sintering Technique. *Ceram. Int.*, 2016. 42(10): 12312–12322.
12. Paiman. S. H., Rahman. M. A., Othman. M. H. D., Ismail. A. F., Jaafar. J., Aziz. A. A. Morphological study of Yttria-Stabilized Zirconium Hollow Fibre Membrane Prepared using Phase Inversion/Sintering Technique. *Ceram. Int.*, 2015. 41(10): 12543–12553.
13. Wei. C. C., Chen. O. Y., Liu. Y., Li. K. Ceramic asymmetric Hollow Fibre Membranes—One Step Fabrication Process. *J. Memb. Sci.*, 2008. 320(1–2): 191–197.
14. Tan. X., Wang. Z., Li. K. Effects of Sintering on the Properties of $La_{0.6}Sr_{0.4}Co_{0.2}Fe_{0.8}O_{3-\delta}$ Perovskite Hollow Fiber Membrane. *Ind. Eng. Chem. Res.*, 2010. 49: 2895–2901.
15. Tan. X., Li. K. Inorganic Hollow Fibre Membranes in Catalytic Processing. *Curr. Opin. Chem.*, 2011. 1(1): 69–76.
16. Abdullah. N., Rahman. M. A., Othman. M. H. D, Ismail. A. F., Jaafar. J. Preparation and characterization of Dual Layer Thin Layer Lanthanum Strontium Cobalt Ferrite /Alumina Hollow Fiber Membrane using Dip-coating and Brush-coating Techniques. *Sains Malaysiana.*, 2016. 45(11): 1715–1721.
17. Droushiotis. N., Doraswami. U., Ivey. D., Othman. M. H. D., Li. K., Kelsall. G. Fabrication by Co-extrusion and electrochemical characterization of Micro-Tubular Hollow Fibre Solid Oxide Fuel Cells. *Electrochem. Commun.*, 2010. 12(6): 792–795.
18. García-García. F. R, Tsang. S. C., Li. K. Hollow Fibre Based Reactors for an Enhanced H_2 Production by Methanol Steam Reforming. *J. Memb. Sci.*, 2014. 455: 92–102.
19. Rahman. M. A., García-García. F. R., Li. K. Development of a catalytic hollow fibre membrane microreactor as a microreformer unit for Automotive Application. *J. Memb. Sci.*, 2012. 390–391: 68–75.
20. Liu. X., Demir. N. K., Wu. Z., Li. K. Highly Water-Stable Zirconium Metal-Organic Framework UiO-66 Membranes Supported on Alumina Hollow Fibers for Desalination. *J. Am. Chem. Soc.*, 2015. 137(22): 6999–7002.

21. Wang. C., Lee. M., Liu. X., Wang. B., Paul. C. J., Li. K. A metal-organic framework/α-alumina composite with a novel geometry for Enhanced Adsorptive Separation. *Chem. Commun.*, 2016. 52(57): 8869–8872.

22. Friebe. S., Geppert. B., Steinbach. F., Caro. J. Metal-Organic Framework UiO-66 Layer: A Highly Oriented Membrane with Good Selectivity and Hydrogen Permeance. *Appl. Mater. Interfaces.*, 2017. 9(14): 12878–12885.

23. Dey. C., Kundu. T. Crystal Engineering Crystalline Metal-Organic Frameworks (Mofs): Synthesis , Structure and Function. *Acta. Crystallogr.*, 2014. 70: 3–10.

24. Greathouse. J. A., Allendorf. M. D. The Interaction of Water with MOF-5 Simulated by Molecular Dynamics. *J. Am. Chem. Soc.*, 2006. 128(33): 10678–10679.

25. Wang. C., Liu. X., Demir. K., Paul. J., Li. K. Applications of Water Stable Metal – Organic Frameworks. *Chem. Soc. Rev.*, 2016. 45: 5107-5134.

26. Leus. K., Bogaerts. T., De. D. J., Depauw. H., Hendrickx. K., Vrielinck. H, et al. Systematic Study of the Chemical and Hydrothermal Stability of Selected "Stable" Metal Organic Frameworks. *Microporous Mesoporous Mater.*, 2016. 226:110–116.

27. Katz. M. J., Moon. S. Y., Mondloch. J. E., Beyzavi. M. H., Stephenson. C. J., Hupp. J. T., et al. Exploiting Parameter Space in MOFs: A 20-Fold Enhancement of Phosphate-Ester Hydrolysis with UiO-66-NH_2. *Chem. Sci.*, 2015. 6(4): 2286–2291.

28. Rowsell. J. L. C., Yaghi. O. M. Metal – organic frameworks : A new Class of Porous Materials. *Microporous Mesoporous Mater.*, 2004. 73: 3–14.

29. Stock. N., Biswas. S. Synthesis of Metal-Organic Frameworks (MOFs): Routes to Various MOF Topologies, Morphologies, and Composites. *J. Am. Chem. Soc.*, 2012. 112: 933–969.

30. Zhao. Y., Song. Z., Li. X., Sun. Q., Cheng. N., Lawes. S., et al. Metal Organic Frameworks for Energy Storage and Conversion. *Energy Storage Mater.*, 2016. 2: 35–62.

31. Kadhom. M., Hu. W., Deng. B. Thin film Nanocomposite Membrane Filled with Metal-Organic Frameworks UiO-66 and MIL-125 Nanoparticles for Water Desalination. *Membranes.*, 2017. 7(2): 1-16.

32. Sutrisna. P. D., Hou. J., Zulkifli. M. Y., Li. H., Zhang. Y., Liang. W., et al. Surface Functionalized Uio-66/Pebax-Based Ultrathin Composite Hollow Fiber Gas Separation Membranes. *J. Mater. Chem. A*, 2018. 6: 918-931.

33. Molavi. H., Shojaie. A., Mousavi. S. A.. Improving Mixed-Matrix Membrane Performance via PMMA Grafting from Functionalized. *J. Mater. Chem. A Mater.*, 2018. 6: 2775–2791.

34. Ranjan. R., Tsapatsis. M. Microporous Metal Organic Framework Membrane on Porous Support using the Seeded Growth Method. *Chem. Mater.*, 2009. 21(20): 4920–4924.

35. Zhou. S., Zou. X., Sun. F., Zhang. F., Fan. S., Zhao. H, et al. Challenging Fabrication of Hollow Ceramic Fiber Supported $Cu_3(BTC)_2$ Membrane for Hydrogen Separation. *J. Mater. Chem.*, 2012. 22(20): 10322.

36. Nan. J., Dong. X., Wang. W., Jin. W., Xu. N. Step-by-Step Seeding Procedure for Preparing HKUST-1 Membrane on Porous r -Alumina Support. *Langmuir.*, 2011. 27: 4309–4312.

37. Centrone. A., Yang. Y, Speakman. S., Bromberg. L., Rutledge. G. C., Hatton. T. A. Growth of Metal - Organic Frameworks on Polymer Surfaces. *J. Am. Chem. Soc.*, 2010. 132(25): 15687–15691.

38. Fan. S., Wu. S., Liu. J., Liu. D. Fabrication of MIL-120 Membranes Supported by α-Al_2O_3 Hollow Ceramic Fibers for H_2 Separation. *RSC Adv.*, 2015. 5: 54757–54761.

39. Zhang. X., Liu. Y., Kong. L., Liu. H., Qiu. J., Han. W., et al. A Simple and Scalable Method for Preparing Low-Defect ZIF-8 Tubular Membranes. *J. Mater. Chem. A.*, 2013. 1(36): 10635–10638.

40. Chen. Y., Li. S., Pei. X., Zhou. J., Feng. X., Zhang. S., et al. A Solvent-Free Hot-Pressing Method for Preparing Metal-Organic-Framework Coatings. *Angew. Chemie - Int. Ed.*, 2016. 55(10): 3419–3423.

41. Muhammad. N., Abdullah. N., Zahir. M. P. M., Rahman. M. A., Abas. K. H., et al. Synthesis and Performance Evaluation of Zeolitic Imidazolate Framework-8 Membranes Deposited onto Alumina Hollow Fiber for Desalination. *Korean J. Chem. Eng.*, 2018. 35(3): 1–11.

42. Zhang. H., Hou. J., Hu. Y., Wang. P., Ou. R., Jiang. L., et al. Ultrafast selective transport of alkali metal ions in metal organic frameworks with subnanometer pores. *Sci. Adv.*, 2018. 4(2): 1-8.

43. Fang. H., Gao. J. F., Wang. H. T., Chen. C. S. Hydrophobic Porous Alumina Hollow Fiber for Water Desalination via Membrane Distillation Process. *J. Mem.b Sci.*, 2012. 403–404: 41–46.

44. Wan. L., Zhou. C., Xu. K., Feng. B., Huang. A. Synthesis of Highly Stable UiO-66-NH_2 Membranes with High Ions Rejection for Seawater Desalination. *Microporous Mesoporous Mater.*, 2017. 252: 207–213.

45. Wu. F., Lin. L., Liu. H., Wang. H,., Qiu. J., Zhang. X. Synthesis of Stable UiO-66 Membranes for Pervaporation Separation of Methanol/Methyl tert-butyl ether Mixtures by Secondary Growth. *J. Memb. Sci.*, 2017. 544: 342–350.

46. Wu. F., Cao. Y., Liu. H., Zhang. X. High-performance UiO-66-NH_2 Tubular Membranes by Zirconium-Induced Synthesis for Desulfurization of Model Gasoline via Pervaporation. *J. Memb. Sci.*, 2018. 556: 54–65.

47. Bhatnagar. A., Sillanpää. M. Removal of Natural Organic Matter (NOM) and Its Constituents from Water by Adsorption – A Review. *Chemosphere.*, 2017. 166: 497–510.

48. Ibrahim. N. and Aziz. H. A. Trends on Natural Organic Matter in Drinking Water Sources and its Treatment. *Int. J. Sci. Res. Environ. Sci.*, 2014. 2(3): 94–106.

49. Boretti. A., Rosa. L. Reassessing the Projections of the World Water Development Report. *NPJ Clean Water.*, 2019. 2(15): 1-5.

50. Lin. K. Y. A., Chang. H. A. Efficient Adsorptive Removal of Humic Acid from Water using Zeolitic Imidazole Framework-8 (ZIF-8). *Water Air Soil Pollut.*, 2015. 226(2): 1-17.

51. Qin. X., Liu. F., Wang. G. Adsorption of Humic Acid from Aqueous Solution by Hematite : Effects of pH and Ionic Strength. *Environ. Earth Sci.*, 2015. 73: 4011–4017

52. Song. H., Shao. J., He. Y., Liu. B., Zhong. X. Natural Organic Matter Removal and Flux Decline with PEG-TiO_2-doped PVDF Membranes by Integration of Ultrafiltration with Photocatalysis. *J. Memb. Sci.*, 2012. 405–406: 48–56.

53. Academy of Science Malaysia, *Study on the current issues and needs for water supply and wastewater management in Malaysia.*Volume 2. Academy of Science Malaysia. 2015.

54. Giasuddin. A. B. M., Kanel. S. R., Choi. H. Adsorption of Humic Acid onto Nanoscale Zerovalent Iron and Its Effect on Arsenic Removal. *Environ. Sci. Technol.*, 2007. 41(6): 2022–2027.

55. Doulia. D., Leodopoulos. C., Gimouhopoulos. K., Rigas. F. Adsorption of Humic Acid on Acid-Activated Greek Bentonite. *J. Colloid Interface Sci.*, 2009. 340(2): 131–141.

56. Tang. Y., Liang. S., Yu. S., Gao. N., Zhang. J., Guo. H., et al. Enhanced Adsorption of Humic Acid on Amine Functionalized Magnetic Mesoporous Composite Microspheres. *Colloids Surfaces A Physicochem Eng Asp.*, 2012. 406: 61–67.

57. Chu. K. H., Huang. Y., Yu. M., Heo. J., Flora. J. R. V., Jang. A., Jang. M., et al. Evaluation of Graphene Oxide-Coated Ultrafiltration Membranes for Humic Acid Removal at Different Ph and Conductivity Conditions. *Sep. Purif Technol.*, 2017. 181: 139–147.

58. Bruggen. B. V. D. and Vandecasteele. C. Removal of Pollutants From Surface Water and Groundwater by Nanofiltration: Overview of Possible Applications in the Drinking Water Industry. *Environ. Pollut.*, 2003. 122(3): 435–445.

59. Sablani. S., Goosen. M., Al-Belushi. R., Wilf. M. Concentration Polarization in Ultrafiltration and Reverse Osmosis: A Critical Review. *Desalination.*, 2001. 141(3): 269–289.

60. Marchese. J., Ponce. M., Ochoa. N. A., Prádanos. P., Palacio. L., Hernández. A. Fouling Behaviour of Polyethersulfone UF Membranes Made with Different PVP. *J. Memb. Sci.*, 2003. 211: 1–11.

61. Yuan. W., Zydney. A. L. Humic Acid Fouling during Ultrafiltration. *Environ. Sci. Technol.*, 2000. 34(23): 5043–5050.

62. Hwang. K. J., Lin. T. T. Effect of Morphology of Polymeric Membrane on the Performance of Cross-Flow Microfiltration. *J. Memb. Sci.*, 2002. 199(1–2): 41–52.

63. Barros. S. T. D., Andrade. C. M. G., Mendes. E. S., Peres. L. Study of Fouling Mechanism in Pineapple Juice Clarification by Ultrafiltration. *J. Memb. Sci.*, 2003. 215(1–2): 213–224.

64. Baker. R. W. *Membrane Technology and Applications*. 3rd ed. Chichester, UK: John Wiley and Sons; 2012.

65. Xia. S., Zhou. Y., Ma. R., Xie. Y., Chen J. Ultrafiltration of Humic Acid and Surface Water with Tubular Ceramic Membrane. *Desalin. Water Treat.*, 2013. 51(25–27): 5319–5326.

66. Mänttäri. M,. Puro. L., Nuortila. J. J., Nyström. M. Fouling Effects of Polysaccharides and Humic Acid in Nanofiltration. *J. Memb. Sci.*, 2000. 165(1): 1–17.

67. Srisurichan. S., Jiraratananon. R., Fane. A. G. Humic Acid Fouling in the Membrane Distillation Process. *Desalination.*, 2005. 174(1): 63–72.

68. Thuyavan. Y. L., Anantharaman. N., Arthanareeswaran. G. Adsorptive Removal of Humic Acid by Zirconium Embedded in a 2Poly (ether sulfone) Membrane. *Ind. Eng. Chem. Res.*, 2014. 53: 11355–11364.

69. Kumar. M., Gholamvand. Z., Morrissey. A., Nolan. K., Ulbricht. M., Lawler. J. Preparation and Characterization of Low Fouling Novel Hybrid Ultrafiltration Membranes Based on the Blends of GO-TiO_2 Nanocomposite and Polysulfone for Humic Acid Removal. *J. Memb. Sci.*, 2016. 506: 38–49.

70. Teow. Y. H., Ooi. B. S., Ahmad. A. L. Study on PVDF-TiO_2 Mixed-Matrix Membrane Behaviour Towards Humic Acid Adsorption. *J. Water Process Eng.*, 2017. 15: 99–106.

71. Son. M., Kim. H., Jung. J., Jo. S., Choi. H. Influence of Extreme Concentrations of Hydrophilic Pore-Former on Reinforced Polyethersulfone Ultrafiltration Membranes for Reduction of Humic Acid Fouling. *Chemosphere.*, 2017. 179: 194–201.

72. Teow. Y. H., Ooi. B. S., Ahmad. A. L. Fouling Behaviours of PVDF-TiO_2 Mixed-Matrix Membrane Applied to Humic Acid Treatment. *J. Water Process Eng.*, 2017. 15: 89–98.

73. Rahman. M. A., Kingsbury. B. F. K., Li. K. A Novel Catalytic Membrane Microreactor for CO_x Free H_2 Production. *Catal. Commn.*, 2010. 12: 161–164.

74. Rahman. M. A., García-García. F. R., Li. K. On-board H_2 Generation by A Catalytic Hollow Fibre Microreactor for Portable Device Applications. *Catal. Commun.*, 2011. 16(1): 128–132.

75. Wu. Z., Wang. B., Li. K. A Novel Dual-Layer Ceramic Hollow Fibre Membrane Reactor for Methane Conversion. *J. Memb. Sci.*, 2010. 352(1–2): 63–70.

76. Othman. N. H., Wu. Z., Li. K. Functional Dual-Layer Ceramic Hollow Fibre Membranes for Methane Conversion. *Procedia Eng.*, 2012. 44: 1484–1495.

77. Wu. Z., Wang. B., Li. K. Functional LSM-ScSZ/NiO-ScSZ Dual-Layer Hollow Fibres for Partial Oxidation of Methane. *Int. J. Hydrogen Energy.*, 2011. 36(9): 5334–5341.

78. Wang. J., Wen. F. Y., Zhang. Z. H., Zhang. X. D., Pan. Z. J., Zhang. P., et al. Investigation on Degradation of Dyestuff Wastewater using Visible Light in the Presence of a Novel Nano TiO_2 Catalyst Doped with Upconversion Luminescence Agent. *J. Photochem. Photobiol. A. Chem.*, 2006. 180(1–2): 189–195.

79. Othman. M. H. D., Wu. Z., Droushiotis. N., Kelsall. G., Li. K. Morphological Studies of Macrostructure of Ni-CGO Anode Hollow Fibres for Intermediate Temperature Solid Oxide Fuel Cells. *J. Memb. Sci.*, 2010. 360: 410–457.

80. Othman. M. H. D., Droushiotis. N., Wu. Z., Kanawka. K., Kelsall. G., Li. K. Electrolyte Thickness Control and Its Effect on Electrolyte/Anode Dual-Layer Hollow Fibres for Micro-Tubular Solid Oxide Fuel Cells. *J. Memb. Sci.*, 2010. 365:382–398.

81. Droushiotis. N., Torabi. A., Othman. M. H. D, Etsell. T. H., Kelsall. G. H. Effects of Lanthanum Strontium Cobalt Ferrite (LSCF) Cathode Properties on Hollow Fibre Micro-Tubular SOFC Performances. *J. Appl. Electrochem.*, 2012. 42: 517–526.

82. Li. T., Wu. Z., Li. K. Single-Step Fabrication and Characterisations of Triple-Layer Ceramic Hollow Fibres for Micro-Tubular Solid Oxide Fuel Cells (SOFCs). *J. Memb. Sci.*, 2014. 449: 1–8.

83. Li. K. *Ceramic Membranes for Separation and Reaction.* John Wiley & Sons Ltd, The Atrium, Southern Gate, Chichester. 2007.

84. Jamil. S. M., Hafiz. M. O. D., Rahman. M. A., Jaafar. J., Ismail. A. F., et al. Recent Fabrication Techniques for Micro-Tubular Solid Oxide Fuel Cell Support : A Review. *J. Euro. Cer. Soc.*, 2015. 35: 1–22.

85. Lee. M., Wu. Z., Li. K. *Advances in Ceramic Membranes for Water Treatment.* Woodhead Publishing Series in Energy. 43–82. 2015.

86. Lee. D., Zhang. L., Oyama. S. T., Niu. S., Saraf. R. F. Synthesis, Characterization, and Gas Permeation Properties of a Hydrogen Permeable Silica Membrane Supported on Porous Alumina. *J. Memb. Sci.*, 2004. 231(1–2): 117–126.

87. Irfan. H. M. D., Tan. X., Wu. Z., Li. K. Pd/Al_2O_3 Composite Hollow Fibre Membranes: Effect of Substrate Resistances on H_2 Permeation Properties. *Chem. Eng. Sci.*, 2011. 66(6): 1150–1158.

88. Shao. J., Zhan. Z., Li. J., Wang. Z., Li. K., Yan. Y. Zeolite NaA Membranes Supported on Alumina Hollow Fibers: Effect of Support Resistances on Pervaporation Performance. *J. Memb. Sci.*, 2014. 451: 10–17.

89. Aba. N. F. D., Chong. J. Y., Wang. B., Mattevi. C., Li. K. Graphene Oxide Membranes on Ceramic Hollow Fibers - Microstructural Stability and Nanofiltration Performance. *J. Memb. Sci.*, 2015. 484: 87–94.

90. Tseng. H. H., Wang. C. T., Zhuang. G. L., Uchytil. P., Reznickova. J., Setnickova. K. Enhanced H_2/CH_4 and H_2/CO_2 Separation by Carbon Molecular Sieve Membrane Coated on Titania Modified Alumina Support: Effects of TiO_2 Intermediate Layer Preparation Variables on Interfacial Adhesion. *J. Memb. Sci.*, 2016. 510: 391–404.

91. Betke. U., Proemmel. S., Rannabauer. S., Lieb. A., Scheffler. M., Scheffler. F. Silane Functionalized Open-Celled Ceramic Foams as Support Structure in Metal Organic Framework Composite Materials. *Microporous Mesoporous Mater.*, 2017. 239: 209–220.

92. Muhamad. N., Abdullah. N., Rahman. M. A., Abas. K. H., Aziz. A. A. Removal of nickel from aqueous solution using supported zeolite-Y Hollow Fiber Membranes. *Environ. Science and Pollution Res.*, 2018. 25: 19054–19064.

93. Rana. D., Matsuura. T. Surface Modifications for Antifouling Membranes. *Chem. Rev.*, 2010. 110(4): 2448–2471.

94. Ishak. N. F., Hashim. N. A., Othman. M. H. D., Monash. P., Zuki. F. M. Recent Progress in the Hydrophilic Modification of Alumina Membranes for Protein Separation and Purification. *Ceram. Int.*, 2017. 43(1): 915–925.

95. Furukawa. H., Ga. F., Hudson. M. R., Yaghi. O. M. Water Adsorption in Porous Metal − Organic Frameworks and Related Materials. *J. Am. Chem. Soc.*,2014. 136, 4369−4381.

96. Rego. R. M., Kuriya. G., Kurkuri. M. D., Kigga. M. MOF Based Engineered Materials in Water Remediation: Recent Trends. *J. Hazard Mater.*, 2021. 403: 123605.

97. Shekhah. O., Liu. J., Fisrcher. R. A., Woll. C. H. MOF Thin Films: Existing and Future Applications. *Chem Soc Rev.*, 2011. 40(2): 1081–1106.

98. Kumar. S., Jain. S., Nehra. M., Dilbaghi. N., Marrazza. G., Kim. K. H. Green Synthesis of Metal–Organic Frameworks: A State-of-the-art Review of Potential Environmental and Medical Applications. *Coord. Chem. Rev.*, 2020. 420: 213407.

99. Shilun. Qiu., Ming. X., Zhu. G. Metal-Organic Framework Membranes: From Synthesis to Separation Application. *Chem. Soc. Rev.*, 2014. 43: 6116-6140.

100. Batten. M. P., Rubio-Martinez. M., Hadley. T., Carey. K. C., Polyzos. K. S. L. A., Hill. M. R. Continuous Flow Production of Metal-Organic Frameworks. *Curr. Opin. Chem. Eng.*, 2015. 8: 55–9.

101. Denny. M. S.; Moreton. J. C.; Benz. L.; Cohen. S. M. Metal–Organic Frameworks for Membrane-Based Separations. *Nat. Rev. Mat.*, 2016. 1: 1-17.

102. Dias. E. M. and Petit. C. Towards the Use Of Metal–Organic Frameworks For Water Reuse: A Review Of The Recent Advances In The Field Of Organic Pollutants Removal And Degradation And The Next Steps In The Field. *J. Mater. Chem. A*, 2015. 3(45): 22484–22506.

103. Cavka. J. H., Jakobsen. S., Olsbye. U., Guillou. N., Lamberti. C., Bordiga. S., et al. A New Zirconium Inorganic Building Brick Forming Metal Organic Frameworks with Exceptional Stability. *J. Am. Chem. Soc.*, 2008. 130(42): 13850–13851.

104. Vermoortele.. F, Bueken. B., Voorde. B. V. D., Vandichel. M., Houthoofd. K., Vimont. A., et al. Synthesis Modulation as a Tool To Increase the Catalytic Activity of Metal − Organic Frameworks: The Unique Case of UiO-66(Zr). *J. Am. Chem. Soc.*, 2013. 66: 11465–11468.

105. Schaate. A., Roy. P., Godt. A., Lippke. J., Waltz. F., Wiebcke. M., et al. Modulated Synthesis of Zr-Based Metal-Organic Frameworks: From Nano to Single Crystals. *Chem. A Eur. J.*, 2011. 17(24): 6643–6651.

106. Hu. Z., Castano. I., Wang. S., Wang. Y., Peng. Y., Qian. Y., et al. Modulator Effects on the Water-Based Synthesis of Zr/Hf Metal-Organic Frameworks: Quantitative Relationship Studies between Modulator, Synthetic Condition, and Performance. *Cryst. Growth Des.*, 2016. 16(4): 2295–2301.

107. Jiao. Y., Liu. Y., Zhu. G., Hungerford. J. T., Bhattacharyya. S., Lively. R. P., et al. Heat-Treatment of Defective UiO-66 from Modulated Synthesis: Adsorption and Stability Studies. *J. Phys. Chem. C.*, 2017. 121(42): 23471–23479.

108. Forgan. R. S. Modulated Self-Assembly of Metal-Organic Frameworks. *Chem. Sci.*, 2020. 11(18): 4546–3562.

109. Wu. H., Chua. Y. S., Krungleviciute. V., Tyagi. M., Chen P., Yildirim. T., et al. Unusual and Highly Tunable Missing-Linker Defects in Zirconium Metal – Organic Framework UiO-66 and Their Important Effects on Gas Adsorption. *J. Am. Chem. Soc,*. 2013. 135(28): 10525–10532.

110. Piscopo. C. G., Polyzoidis. A., Schwarzer. M., Loebbecke. S. Stability of UiO-66 Under Acidic Treatment : Opportunities and Limitations for Post-Synthetic modifications. *Microporous Mesoporous Mater.*, 2015. 208: 30–35.

111. Winarta.. J, Shan. B., Mcintyre. S. M., Ye. L., Wang. C., Liu. J., et al. A Decade of UiO-66 Research : A Historic Review of Dynamic Structure , Synthesis Mechanisms , and Characterization Techniques of an Archetypal Metal – Organic Framework. *Cryst. Growth Des.*, 2020. 20(2): 1347–1362.

112. Garibay. S. J., Cohen. S. M. Isoreticular Synthesis and Modification of Frameworks with the UiO-66 Topology. *Chem. Commun.*, 2010. 46: 7700–7782.

113. Cmarik. G. E., Kim. M., Cohen. S. M., Walton. K. S. Tuning the Adsorption Properties of UiO-66 via Ligand Functionalization. *Langmuir,* 2012. 28(44): 15606–15613.

114. Phan. A., Doonan. C. J., Uribe-Romo. F. J., Knobler. C. B., Okeeffe. M., Yaghi. O. M. Synthesis, Structure, and carbon dioxide capture properties of Zeolitic Imidazolate Frameworks. *Acc. Chem. Res.,* 2010. 43(1): 58–67.

115. Valenzano. L., Civalleri. B., Chavan. S., Bordiga. S., Nilsen. M. H., Jakobsen. S., et al. Disclosing the Complex Structure of UiO-66 Metal Organic Framework : A Synergic Combination of Experiment and Theory. *Chem. Mater.*, 2011. 23(7): 1700–1718.

116. Walton. K. S., Snurr. R. Q. Applicability of the BET Method for Determining Surface Areas of Microporous Metal - Organic Frameworks. *J. Am. Chem. Soc.*, 2007. 1129(27): 8552–8556.

117. Bardestani. R., Patience. G. S. and Kaliaguine. S. Experimental Methods in Chemical Engineering: Specific Surface Area and Pore Size Distribution Measurements—BET, BJH, and DFT. *Can. J. Chem. Eng.*, 2019. 97(11): 2781–2791.

118. Abánades Lázaro. I., Haddad. S., Sacca. S., Orellana-Tavra. C., Fairen-Jimenez. D., Forgan. R. S. Selective Surface PEGylation of UiO-66 Nanoparticles for Enhanced Stability, Cell Uptake, and pH-Responsive Drug Delivery. *Chem.*, 2017. 2(4): 561–578.

119. Navarro. A. R., Cirre. L., Carboni. M., Meyer. D. BTEX Removal from Aqueous Solution with Hydrophobic Zr Metal Organic Frameworks. *J. Environ. Manage.*, 2018. 214: 17–22.

120. Wang. Y., Li, L., Dai. P., Yan. L., Cao. L., Gu. X., et al. Missing-Node Directed Synthesis of Hierarchical Pores on a Zirconium Metal-Organic Framework with Tunable Porosity and Enhanced Surface Acidity: Via a Microdroplet Flow Reaction. *J. Mater. Chem. A.*, 2017. 5(42): 22372–22379.

121. Moreira. M. A., Santos. C., Ferreira. A. F. P., Loureiro. J. M., Ragon. F., Horcajada. P., et al. Reverse Shape Selectivity in the Liquid-Phase Adsorption of Xylene Isomers in Zirconium Terephthalate MOF UiO-66. *Lagmuir.*, 2012. 28(13): 5715-5723.

122. Wang. C., Liu. X., Chen. J. P., Li. K. Superior Removal of Arsenic from Water with Zirconium Metal-Organic Framework UiO-66. *Sc.i Rep.*, 2015. 5: 16613.

123. Smith. S. J. D., Ladewig. B. P., Hill. A. J., Lau. C. H., Hill. M. R. Post-synthetic Ti Exchanged UiO-66 Metal-Organic Frameworks that Deliver Exceptional Gas Permeability in Mixed Matrix Membranes. *Sci. Rep.*, 2015. 1: 15–28.

124. Wang. A., Zhou. Y., Wang. Z., Chen. M., Liu. X. Titanium Incorporated with UiO-66(Zr)-type Metal–Organic Framework (MOF) for Photocatalytic Application. *RSC Adv.*, 2016. 6: 3671–3679.

125. Miyamoto. A. M., Hori. K., Goshima. T., et al. An Organoselective Zr-Based Metal Organic Framework UiO-66 Membrane for Pervaporation. *Euro. J. Inorg. Chem.*, 2017. 14: 2094-2099.

126. Sun. Y., Hu. Z., Zhao. D., Zeng. K. Mechanical Properties of Microcrystalline Metal − Organic Frameworks (MOFs) Measured by Bimodal Amplitude Modulated- Frequency Modulated Atomic Force Microscopy. *ACS Appl. Mater. Interfaces.*, 2017. 9(37): 32202–32210.

127. Kolokolov. D. I., Stepanov. A. G., Guillerm. V., Serre. C., Frick. B., Jobic. H. Probing the Dynamics of the Porous Zr Terephthalate UiO-66 Framework using 2H NMR and Neutron Scattering. *J. Phys. Chem. C.*, 2012. 116(22): 12131–12136.

128. Gonzalez-Nelson. A., Coudert. F. X., Veen. M. A. Rotational Dynamics of Linkers in Metal–Organic Frameworks. *Nanomaterials,* 2019. 9(3): 330.

129. Khudozhitkov. A. E., Jobic. H., Kolokolov. D. I, Freude. D., Haase. J., Stepanov. A. G. Probing the Guest-Mediated Structural Mobility in the UiO-66(Zr) Framework by 2H NMR Spectroscopy. *J. Phys. Chem. C.* 2017. 121(21): 11593–11600.

130. Khudozhitkov. A. E., Kolokolov. D. I., Stepanov. A. G. Characterization of Fast Restricted Librations of Terephthalate Linkers in MOF UiO-66(Zr) by 2H NMR Spin-Lattice Relaxation Analysis. *J. Phys. Chem. C.* 2018. 122(24): 12956–12962.

131. Kolokolov. D. I., Jobic. H., Stepanov. A. G., Guillerm. V., Devic. T., Serre. C., et al. Dynamics of Benzene Rings in MIL-53(Cr) and MIL-47(V) Frameworks Studied by 2H NMR Spectroscopy. *Angew. Chemie.*, 2010. 49(28): 4791–4794.

132. Kolokolov. D. I., Stepanov. A. G., Jobic. H. Guest Controlled Rotational Dynamics of Terephthalate Phenylenes in Metal-Organic Framework MIL-53(Al): Effect of Different Xylene Loadings. *J. Phys. Chem. C.* 2014. 118(29): 15978–15984.

133. Liu X. Metal-Organic Framework UiO-66 Membranes. *Front. Chem. Sci. Eng.*, 2020. 14: 216–232.

134. Zuo. Y., Zhang. Z., Wei. Y., Liu. M., Song. C., Guo. X., et al. Facile Synthesis of Morphology and Size-Controlled Zirconium Metal–Organic Framework UiO-66: the Role of Hydrofluoric Acid in Crystallization. *Cryst. Eng. Comm.*, 2015. 17(33): 6434–6440.

135. McGuire. C. V., Forgan. R. S. The Surface Chemistry of Metal–Organic Frameworks. *Chem. Commun.,* 2015. 51(25): 5199–5217.

136. Lyu. Q., Deng. X., Hu. S., Lin. L., Ho. W. S. W. Exploring the Potential of Defective UiO-66 as Reverse Osmosis Membranes for Desalination. *J. Phys. Chem. C.*, 2019. 123: 16118–16126.

137. Miyamoto. M., Kohmura. S., Iwatsuka. H., Oumi. Y., Uemiya. S. In situ Solvothermal Growth of Highly Oriented Zr- Based Metal Organic Framework UiO-66 Film with Monocrystalline Layer. *Cryst. Eng. Comm.*, 2015. 17: 3422–3425.

138. Liu. X., Wang. C., Wang. B., Li. K. Novel Organic-Dehydration Membranes Prepared from Zirconium Metal-Organic Frameworks. *Adv Funct. Mater.* 2017. 27(3): 1–6.

139. Wang. N., Zhang. G., Wang. L., Li. J., An. Q., Ji. S. Pervaporation Dehydration of Acetic Acid using NH_2 -UiO-66/PEI Mixed Matrix Membranes. *Sep. Purif. Technol.*, 2017. 186: 20–27.

140. Huang. K., Wang. B., Guo. S., Li. K. Micropatterned Ultrathin MOF Membranes with Enhanced Molecular Sieving Property. *Angew. Chemie.*, 2018. 57(42): 13892–13896.

141. Li. W., Zhang. Y., Li. Q., Zhang. G. Metal-Organic Framework Composite Membranes: Synthesis and Separation Applications. *Chem. Eng. Sci.*, 2015. 135: 232–257.

142. Hu. Y., Dong. X., Nan. J., Jin. W., Ren. X., Xu. N., et al. Metal-Organic Framework Membranes Fabricated via Reactive Seeding. *Chem. Commun.*, 2011. 47(2): 737–739.

143. Tyagi. B., Sidhpuria. K., Shaik. B., Jasra. R. V. Synthesis of Nanocrystalline Zirconium using Sol-Gel and Precipitation Techniques. *Ind. Eng. Chem. Res.*, 2006. 45(25): 8643–8650.

144. Mishra. A. K. *Sol-gel based nanoceramic materials: Preparation, properties and applications. Sol-gel Based Nanoceramic Materials: Preparation, Properties and Applications*. Springer. 2016.

145. Dimitriev. Y., Ivanova. Y., Iordanova. R. History of Sol-Gel Science and Technology (Review). *J. Uni. Chem. Tech. Metallurgy.*, 2008. 181–92.

146. Davar. F., Hassankhani. A., Loghman-Estarki. M. R. Controllable synthesis of metastable tetragonal zirconium nanocrystals using Citric Acid Assisted Sol-Gel Method. *Ceram. Int.*, 2013. 39(3): 2933–2941.

147. Lin. C., Zhang. C., Lin. J. Phase Transformation and Photoluminescence Properties of Nanocrystalline Zirconium Powders Prepared via the Pechini-Type Sol-Gel Process. *J. Phys. Chem. C.*, 2007. 111(8): 3300–3307.

148. Makhtar. S. N. N. M., Rahman. M. A., Ismail. A. F., Othman. M. H. D, Jaafar. J. Preparation and Characterization of Glass Hollow Fiber Membrane for Water Purification Applications. *Environ. Sci. Pollut. Res.*, 2017. 24(19): 15918–15928.

149. Alem. A., Sarpoolaky. H., Keshmiri. M. Titania Ultrafiltration Membrane: Preparation, Characterization and Photocatalytic Activity. *J. Eur. Ceram. Soc.*, 2009. 29(4): 629–635.

150. Alem. A., Sarpoolaky. H., Keshmiri. M. Sol-Gel Preparation of Titania Multilayer Membrane for Photocatalytic Applications. *Ceram. Int.*, 2009. 35(5): 1837–1843.

151. Jamil. S. M., Othman. M. H. D., Rahman. M. A., and Jaafar. J. Role of lithium oxide as a sintering aid for a CGO electrolyte fabricated via a phase inversion technique. *RSC Adv.*, 2015. 5: 58154–58162.

152. Hasbullah. H., Kumbharkar. S., Ismail. A. F., Li. K. Preparation of Polyaniline Asymmetric Hollow Fiber Membranes and Investigation Towards Gas Separation Performance. *J. Mem. Sci.*, 2011. 366: 116–124.

153. Wang. B., Lai. Z. Finger-like Voids Induced by Viscous Fingering During Phase Inversion of Alumina/PES/NMP Suspensions. *J. Memb. Sci.*, 2012. 405–406: 275–283.

154. Madaeni. S. S., Sedeh. S. N., Nobili. M. D. E. Ultrafiltration of Humic Substances in the Presence of Protein and Metal Ions. *Trans. Porous Media.*, 2006. 65: 469–484.

155. Lausund. K. B., Nilsen. O. All-Gas-Phase Synthesis of Uio-66 through Modulated Atomic Layer Deposition. *Nat. Commun.*, 2016. 7: 1–9.

156. Barma. S., Mandal. B. Effects of Sintering Temperature and Initial Compaction Load on Alpha-Alumina Membrane Support Quality. *Ceram. Int.*, 2014. 40(7): 11299–11309.

157. Lu. G., Cui. C., Zhang. W., Liu. Y., and Huo. F. Synthesis and Self-Assembly of Monodispersed Metal-Organic Framework Microcrystals. *Chem. - An Asian J.*, 2013. 8(1): 69–72.

158. Lozano. L. A., Iglesias. C. M., Faroldi. B. M. C., Ulla. M. A., Zamaro. J. M. Efficient Solvothermal Synthesis of Highly Porous UiO-66 Nanocrystals in Dimethylformamide-Free Media. *J. Mater. Sci.*, 2018. 53(3): 1862–1873.

159. Germann. L. S., Katsenis. A. D., Huskic. I., Julien. P. A., Etter. M., Farha. O. K., et al. Real-Time in Situ Monitoring of Particle and Structure Evolution in the Mechanochemical Synthesis of UiO-66 Metal − Organic Frameworks. *Cryst. Growth Des.*, 2020. 20 (1): 49-54.

160. He. Y., Tang. Y. P., Ma. D., Chung. T. S. UiO-66 Incorporated Thin-Film Nanocomposite Membranes for Efficient Selenium and Arsenic Removal. *J. Memb. Sci.*, 2017. 541: 262–270.

161. Opalinska. A., Malka. I., Dzwolak. W., Chudoba. T., Presz. A., Lojkowski. W. Size-Dependent Density of Zirconium Nanoparticles. *J. Nanotechnol.*, 2015. 6(1): 27–35.

162. Kocjan. A., Logar. M., and Shen. Z. The Agglomeration , Coalescence and Sliding of Nanoparticles , Leading to the Rapid Sintering of Zirconia Nanoceramics. *Scientific Reports.*, 2017. 7: 2541-2549.

163. Lind. M. L., Suk. D. E., Nguyen. T. V., Hoek. E. M. V. Tailoring the Structure of Thin Film Nanocomposite Membranes to achieve seawater RO Membrane Performance. *Environ. Sci. Technol.*, 2010. 44(21): 8230–8235.

164. Singh. R., Sinha. M. K., Purkait. M. K. Stimuli Responsive Mixed Matrix Polysulfone Ultrafiltration Membrane for Humic Acid and Photocatalytic Dye Removal Applications. *Sep. Purif. Technol.*, 2020. 250: 117247.

165. Algamdi. M. S., Alsohaimi. I. H., Lawler. J., Ali. H. M., Aldawsari. A. M., Hassan. H. M. A. Fabrication of Graphene Oxide Incorporated Polyethersulfone Hybrid Ultrafiltration Membranes for Humic Acid Removal. *Sep. Purif. Technol.*, 2019. 223: 17–23.

166. Gebru. K. A., Das. C. Humic Acid Removal using Cellulose Acetate Membranes Grafted with Poly (Methyl methacrylate) and Aminated using Tetraethylenepentamine. *J.Environ. Manage.*, 2018. 217: 600–610.

167. Kumar. M., Gholamvand. Z., Morrissey. A., Nolan. K., Ulbricht. M., Lawler. J. Preparation and Characterization of Low Fouling Novel Hybrid Ultrafiltration Membranes Based on the Blends of GO-TiO_2 Nanocomposite and Polysulfone for Humic Acid Removal. *J. Memb. Sci.*, 2016. 506: 38–49.

LIST OF PUBLICATIONS

Journal with Impact Factor

1. **Norfazliana Abdullah**, Norfadhilatuladha Abdullah, Nur Farha Adlina Nor Azmi, Mukhlis A. Rahman, A.F. Ismail, M. H. D. Othman, Juhana Jaafar, Khairul Hamimah Abas. UiO-66 Membrane Supported onto Alumina Hollow Fiber Prepared using Multiple Crystallization Method. Submitted to Journal of Australian Ceramic Society. 2020. **(Q2, IF = 1.307)**

2. **Norfazliana Abdullah**, Mukhlis A. Rahman, A.F. Ismail, M. H. D. Othman, Juhana Jaafar. Preparation and Characterization of UiO-66 onto Modified Alumina Hollow Fiber Membrane with Sol-Gel Pechini of Zirconium Nanoparticles. Submitted to Journal of Water Process Engineering. 2020. **(Q1, IF = 3.370)**

3. **Norfazliana Abdullah**, Mukhlis A. Rahman, A.F. Ismail, M. H. D. Othman, Juhana Jaafar. Preparation, characterizations and performance evaluations of alumina hollow fiber membrane incorporated with UiO-66 particles for humic acid removal. Journal of Membrane Science. 563 (1): 162-174. 2018. **(Q1, IF = 7.015)**

Indexed Conference Proceeding

1. **Norfazliana Abdullah**, Mukhlis A. Rahman, Mohd Hafiz Dzarfan Othman, Juhana Jaafar and A. F Ismail. Preparation and Characterization of UiO-66 supported on ceramic hollow fiber for water purification. Proceeding of 7th International Graduate Conference on Engineering, Science and Humanities (IGCESH) 13th -15th August 2018. ISBN: 978-967-2171-27-0.

Book Chapter

1. **Norfazliana Abdullah**, Mukhlis A Rahman, Mohd Hafiz Dzarfan Othman, Juhana Jaafar, Ahmad F Ismail. Membranes and Membrane Processes: Fundamentals, Book chapter, Editors: Angelo Basile, Sylwia Mozia and Raffaele Molinari. *Current Trends and Future Developments on (Bio-) Membranes: Photocatalytic Membranes and Photocatalytic Membrane Reactors*. Elsevier Inc. 45:70. 2018. ISBN: 978-0-12-813549-5.